

**DOSE VERIFICATION OF BRASS MESH BOLUS  
FOR CONTRALATERAL BREAST POST-  
MASTECTOMY IN THREE-DIMENSIONAL  
CONFORMAL RADIOTHERAPY TECHNIQUE**

**SAKINAH BINTI BUANG**

**UNIVERSITI SAINS MALAYSIA**

**2023**

**DOSE VERIFICATION OF BRASS MESH BOLUS  
FOR CONTRALATERAL BREAST POST-  
MASTECTOMY IN THREE-DIMENSIONAL  
CONFORMAL RADIOTHERAPY TECHNIQUE**

by

**SAKINAH BINTI BUANG**

**Thesis submitted in fulfilment of the requirements  
for the degree of  
Master of Science**

**September 2023**

## ACKNOWLEDGEMENT

First and foremost, I would like to express my gratitude to Allah SWT for giving me the opportunity and endless help in finishing this research project. This research has led to development of Post Mastectomy Radiation Therapy (PMRT) practice in collaboration of School of Physics, USM, Agensi Nuklear Malaysia, Bangi, Institut Kanser Negara, Putrajaya and IPPT USM, Kepala Batas with introduction of new bolus material. A special gratitude goes out to all in the team – The Medical Physics and SSDL (Secondary Standard Dosimetry Lab) team Agensi Nuklear Malaysia, Pn Noriza Isa and all the team, the Medical Physics team Institut Kanser Negara, Pn Mahzom Pawancheck and the Medical Physics department IPPT USM Kepala Batas, Dr Mohd Zahri and team. A special appreciation to main supervisor, Dr Nik Noor Ashikin and co-supervisor's Dr Mohd Zahri and Dr Nurul Hashikin, for the commitment, guidance, and continuous support in overcoming numerous obstacles in finishing this research during pandemic COVID-19. I am also grateful to my research member team, for their feedback sessions, and moral support. Lastly, I would be remiss in not mentioning my family. Their belief in me has kept my spirits and motivation high during this process.

## TABLE OF CONTENTS

<b>ACKNOWLEDGEMENT</b> .....	<b>ii</b>
<b>TABLE OF CONTENTS</b> .....	<b>iii</b>
<b>LIST OF TABLES</b> .....	<b>viii</b>
<b>LIST OF FIGURES</b> .....	<b>x</b>
<b>LIST OF SYMBOLS</b> .....	<b>xiv</b>
<b>LIST OF ABBREVIATIONS</b> .....	<b>xvi</b>
<b>LIST OF APPENDICES</b> .....	<b>xxi</b>
<b>ABSTRAK</b> .....	<b>xxii</b>
<b>ABSTRACT</b> .....	<b>xxiv</b>
<b>CHAPTER 1 INTRODUCTION</b> .....	<b>1</b>
1.1 Background of Study.....	1
1.2 Problem Statement .....	3
1.3 Research Objectives .....	5
1.4 Research Significance .....	6
1.5 Scope and Limitation of the Research.....	6
1.6 Outline of thesis .....	7
<b>CHAPTER 2 LITERATURE REVIEW</b> .....	<b>8</b>
2.1 Post-Mastectomy Radiotherapy (PMRT).....	8
2.1.1 Anatomy of Breast .....	8
2.1.2 PMRT Treatment Indication, Prescription and Radiotherapy Techniques .....	10
2.1.3 Dosimetry Planning (Tissue Inhomogeneity Correction) and Three-Dimensional Conformal Radiation Therapy (3DCRT) Treatment Planning .....	12
2.1.4 Bolus.....	15
2.1.4(a) Bolus Material .....	16

	2.1.4(b) Bolus Technique .....	18
2.1.5	Plan Dose Evaluation .....	18
	2.1.5(a) Dose Coverage of Planning Target Volume (PTV) and Organ at Risk (OAR) .....	18
	2.1.5(b) Dose Volume Histogram (DVH) .....	21
	2.1.5(c) Homogeneity Index (HI).....	22
2.2	Radiological and Physical Properties of Brass Mesh Bolus .....	24
	2.2.1 Mass Density and Electron Density .....	24
	2.2.2 CT Number.....	25
	2.2.3 Attenuation Coefficients .....	27
	2.2.3(a) Mass Attenuation Coefficient .....	27
	2.2.3(b) Energy Absorption Coefficient.....	28
2.3	Dosimetric Properties of Brass Mesh Bolus .....	29
	2.3.1 Percentage Depth Dose (PDD).....	29
	2.3.2 Build-Up Dose and Kerma.....	31
	2.3.3 Surface Dose .....	34
2.4	Radiation Dosimeter.....	36
	2.4.1 NanoDot™ .....	36
	2.4.1(a) NanoDot™ Irradiation .....	37
	2.4.2 Radiation Detectors .....	38
	2.4.2(a) Ionization Chamber and Electrometers .....	39
	2.4.2(b) Geiger–Müller Counters .....	40
	2.4.3 Dosimetry Properties.....	42
	2.4.3(a) Linearity Dose Response .....	42
	2.4.3(b) Angular Dependence .....	43
	<b>CHAPTER 3 METHODOLOGY.....</b>	<b>45</b>
3.1	Calibration and Characterization of the Dosimeter.....	47

3.1.1	Characterization of the Dosimeter in Corresponding to Cobalt-60 Energy .....	47
3.1.1(a)	Ludlum Detector System .....	47
3.1.1(b)	NanoDot™ and Ionization Chamber (IC) .....	48
3.1.2	Characterization of the Dosimeter in Corresponding to Megavoltage (MV) Energy .....	50
3.1.2(a)	Linearity .....	50
3.1.2(b)	Angular Dependence .....	51
3.1.3	NanoDot™ Readout Procedure.....	52
3.2	Radiological, Physical and Dosimetric Properties of Brass Mesh Bolus.....	53
3.2.1	Mass Attenuation Coefficient ( $\mu/\rho$ ) .....	53
3.2.1(a)	Experimental.....	53
3.2.1(b)	XCOM .....	55
3.2.1(c)	GATE.....	55
3.2.2	Mass-Energy Absorption Coefficient ( $\mu_{en}/\rho$ ).....	57
3.2.3	Mass Density .....	58
3.2.3(a)	Conventional Density Method.....	58
3.2.3(b)	HU Number from Electron Density Phantom and Computed Tomography .....	59
3.2.3(c)	Application of Image J Software .....	61
3.2.4	Percentage Depth Dose (PDD), Build-up Region and Surface Dose Dosimetric Analysis.....	63
3.3	Brass Mesh Bolus Application in Post-Mastectomy Radiotherapy (PMRT). 65	
3.3.1	Radiotherapy Simulation.....	65
3.3.1(a)	Phantom Simulation with CT Simulator.....	65
3.3.1(b)	Image Registration.....	67
3.3.1(c)	Contouring .....	68
3.3.2	Treatment Planning .....	69

3.3.2(a)	Dosimetry Planning: Establishment of Brass Relative Electron Density-Curve.....	69
3.3.2(b)	3D Conformal Radiation Therapy (3DCRT).....	72
3.3.3	QA & Treatment Delivery.....	76
3.3.3(a)	Phantom Reproducibility.....	76
3.3.3(b)	Irradiation: NanoDot™ vs TPS dose.....	77
3.3.4	Analysis of High-Risk Organ at Risk (OAR).....	78
<b>CHAPTER 4</b>	<b>RESULTS AND DISCUSSION.....</b>	<b>80</b>
4.1	Calibration and Characterization of the Dosimeter.....	80
4.1.1	Characterization of Dosimeter in Corresponding to Cobalt-60 Energy.....	80
4.1.1(a)	Ludlum detector system.....	80
4.1.1(b)	NanoDot™ and Ionization Chamber.....	82
4.1.2	Characterization of Dosimeter in Corresponding to Megavoltage (MV) Energy.....	83
4.1.2(a)	Ionization Chamber.....	83
4.1.2(b)	NanoDot™.....	84
4.2	Radiological, Physical and Dosimetric Properties of Brass.....	89
4.2.1	Mass Attenuation Coefficient ( $\mu/\rho$ ).....	89
4.2.2	Mass-Energy Absorption Coefficient ( $\mu_{en}/\rho$ ).....	93
4.2.3	Mass Density.....	95
4.2.4	Percentage Depth Dose (PDD).....	101
4.2.5	Build-up Region and Surface Dose.....	103
4.3	Brass Mesh Bolus Application in Post-Mastectomy Radiotherapy (PMRT) .....	104
4.3.1	Dosimetry Planning: Establishment of Brass Relative Electron Density-curve.....	105
4.3.2	3D Conformal Radiation Therapy (3DCRT).....	109
4.3.3	Plan Review and Evaluation.....	110

4.3.3(a)	Dose Volume Histogram (DVH).....	111
4.3.3(b)	Planning Target Volume (PTV) Coverage .....	114
4.3.3(c)	Dose Homogeneity Index (HI) .....	115
4.3.4	QA & Treatment Delivery.....	116
4.3.4(a)	Phantom Reproducibility .....	116
4.3.4(b)	Irradiation: NanoDot™ vs TPS Dose .....	118
4.3.5	Analysis of High-Risk Organ at Risk (OAR).....	119
4.3.5(a)	Contralateral Breast .....	119
4.3.5(b)	Heart .....	120
<b>CHAPTER 5 CONCLUSION AND FUTURE RECOMMENDATIONS....</b>		<b>121</b>
5.1	Conclusion.....	121
5.2	Future Research Recommendations .....	122
<b>REFERENCES.....</b>		<b>124</b>
<b>APPENDICES</b>		



## LIST OF TABLES

		<b>Page</b>
Table 2.1	Literature review summary of brass material.....	17
Table 2.2	Definition of volume in accordance with ICRU 50 and 62. ....	19
Table 3.1	Draft measurement for $\mu_{en}/\rho$ . ....	57
Table 3.2	EDP Plug information's .....	60
Table 3.3	Acquisition criterion for the CT number technique .....	60
Table 3.4	Function of Image J and software features .....	62
Table 3.5	Margin application in contouring brass mesh bolus. ....	68
Table 4.1	Comparison of calculated linear attenuation coefficient, $\mu$ (cm-1) from the mass attenuation coefficient XCOM program.....	91
Table 4.2	Relative differences value of $\mu/\rho$ in different methodology. ....	92
Table 4.3	Comparison $\mu_{en}/\rho$ value by experimental and XCOM.....	95
Table 4.4	Measurement of density by conventional method .....	95
Table 4.5	HU number by computed tomography data .....	96
Table 4.6	Paired sample T-test results for CT analysis and conventional density estimation .....	97
Table 4.7	MPV analysis by Image J software.....	98
Table 4.8	Various density analyses of the brass rod's density. ....	99
Table 4.9	Results of several density methodologies' ANOVA analysis .....	100
Table 4.10	Percentage Depth Dose (PDD) for different bolus application.....	101
Table 4.11	Build-Up and Surface absorbed dose for different bolus application .....	104
Table 4.12	Correcting for position of cheese phantom material plug - Dependent Errors .....	105

Table 4.13	Current standard Electron Density against Hounsefield Number at 120 kVp.....	106
Table 4.14	Brass bolus CT, HU to RED conversion.....	108
Table 4.15	DVH statistics of right chest wall plan with brass mesh bolus.....	111
Table 4.16	DVH of right chest wall plan with superflab bolus statistics.....	112
Table 4.17	Dose distributions as separate bolus application.....	114
Table 4.18	Dose Homogeneity Index for different bolus study.....	116
Table 4.19	Table error for phantom reproducibility evaluation.....	118
Table 4.20	Dose difference in NanoDot™ and Monaco Dose for different bolus application .....	119
Table 4.21	V25 Gy for different bolus application .....	120

## LIST OF FIGURES

	<b>Page</b>
Figure 2.1	9
a) Lymphatic drainage of breast diagram. b) CT images in transverse plan of left breast with lymph nodes position. AV, axillary vessels; Pm, pectoralis minor; PM, pectoralis major; IP, inter-pectoral nodes .....	
Figure 2.2	23
Dose homogeneity and dose conformity relationship .....	
Figure 2.3	30
Percentage depth dose measurement representation .....	
Figure 2.4	31
Dose accumulation from a megavoltage photon beam model .....	
Figure 2.5	33
Absorbed dose or Kerma against depth for MV photon .....	
Figure 2.6	36
On the right side is an active layer white disc in an open form, while on the left is an OSLD encased in a light tight shell .....	
Figure 2.7	37
Mechanism of OSL process during irradiation and readout state. ....	
Figure 2.8	39
Conceptual diagram of Farmer chamber element .....	
Figure 2.9	41
Regions of operation of a gas filled detector. Region E is the GM region. Curve (a) represents 1 MeV beta particles and curve (b) for 100 keV beta particles .....	
Figure 2.10	43
Dosimetry response characteristics (Podgoršak, 2016) .....	
Figure 2.11	44
Angular dependence measurement schematic setup. ....	
Figure 3.1	46
Research work overview .....	
Figure 3.2	49
Setup measurement for measurement of Kerma in air for Cobalt-60.....	
Figure 3.3	50
Calibration of NanoDots <sup>TM</sup> setup.....	
Figure 3.4	51
Linearity and angular dependence measurement of ionization chamber setup.....	
Figure 3.5	52
Linearity and angular dependence measurement of nanoDots <sup>TM</sup> setup .....	

Figure 3.6	Schematic set-up of mass attenuation coefficient measurement a) Measurement of current activity of radioactive sources by dose calibrator b) Measurement of linear attenuation coefficient .....54
Figure 3.7	Flowchart of GATE study for mass attenuation coefficient measurement .....56
Figure 3.8	GATE plot for measuring mass attenuation coefficient. ....56
Figure 3.9	Measurement of $\mu_{en}/\rho$ , for brass alloy samples.....58
Figure 3.10	a) Assemble the EDP phantom. b) Scan EDP using a set of CT energy: 120 kVp; tube current: 250 mAs, in accordance with the upper chest protocol. a calibration curve plot (HU number against density). c) Take out the bone plug and place in a brass plug. step (b) repeated. d) CT number were recorded from CT image. ....61
Figure 3.11	(a) Select "open" from the "File" tab to load the DCM format. (b) Select the ellipse tool to determine the image's grayscale. (c) Note the value for "Mean" in the "Result" window.....62
Figure 3.12	a) 10 pieces of slab water phantom both upper and lower were placed on LINAC couch at FSD=100 cm and align according to laser indicator. b) Output measurement was conducted by ionization chamber and electrometer. c) Pre-irradiation procedure of nanodot .....64
Figure 3.13	Standard radiotherapy treatment workflow .....65
Figure 3.14	a) Phantom was placed on breast board inclined at level 2. b) Ball bearing was placed at origins; three sites on the phantom: right lateral, left lateral and anterior as a marker later for planning and irradiation process. ....66
Figure 3.15	Interface of XiO treatment planning system for OARs (organ at risk) contouring process. ....69
Figure 3.16	a) Position the phantom's solid water plugs ( $\rho=1.000 \text{ g/cm}^3$ ) in the inner radius holes as shown in figure above. b) Plugs were arranged and evenly distribute the high-density tissue throughout the phantom to minimize the artifacts as suggested in Figure 3.17 (a)....71

Figure 3.17	a) Suggestion for plug positioning by Gammex 467 phantom manufacturer b) HU readout procedure for Gammex 467 phantom ..	71
Figure 3.18	Workflow of PTV target coverage assessment. ....	75
Figure 3.19	Process of phantom reproducibility test.....	77
Figure 3.20	a) Irradiation of phantom with superflab bolus b) Brass mesh bolus application for irradiation procedure.....	78
Figure 3.21	Process details of OARs review.....	79
Figure 4.1	Operating voltage for gamma scintillator at average energy of Cobalt-60.....	80
Figure 4.2	Energy response for Ludlum Gamma Scintillator 44-17 Model.....	82
Figure 4.3	NanoDot™ and Ionization calibration curve .....	83
Figure 4.4	Ionization chamber against LINAC output calibration curve .....	84
Figure 4.5	NanoDot™ calibration curve for 6 MV photon beam .....	85
Figure 4.6	Dose response for cylindrical ionization chamber .....	87
Figure 4.7	Dose response for NanoDot™ dosimeter .....	88
Figure 4.8	Relative dose response of NanoDot™ and ionization chamber with respect to angle.....	89
Figure 4.9	Linear attenuation of brass alloy by experimental and GATE study .....	91
Figure 4.10	Absorbed dose against variations of absorber thickness sample .....	94
Figure 4.11	CT density calibration curve of the plug phantoms .....	97
Figure 4.12	Density against MPV by ImageJ.....	99
Figure 4.13	PDD variation as a function of depth for different types of bolus application .....	102
Figure 4.14	HU and RED relationship as the application of Gammex phantom correction.....	107
Figure 4.15	Extrapolation of RED curve correlated with brass .....	108
Figure 4.16	SPV for right chest wall brass bolus at axial plane.....	109

Figure 4.17	BEV for right chest wall brass bolus of anterior view .....	110
Figure 4.18	Brass mesh bolus DVH corresponding to PTV as dose (cGy) function: OAR a) brass bolus b) PTV c) right lung d) patient e) heart f) left lung.....	112
Figure 4.19	Superflab bolus DVH corresponding to a PTV as dose (%) function: OAR: a) skin b) left lung c) heart d) right lung e) PTV ...	113
Figure 4.20	Dose coverage of a) brass mesh bolus b) superflab bolus .....	115

## LIST OF SYMBOLS

A	Area
GeV	Giga electron volt
$K_{\text{air}}$	Kerma in air
$N_k$	Ionization chamber calibration coefficient factor
R	Range
$K_{\text{TP}}$	Temperature and pressure correction factor
$\mu_{\text{en}}/\rho$	Mass energy absorption coefficient
V	Voltage
mGy	miliGray
$\Psi$	Fluence
$D_p$	Prescribed dose
$D_{\text{near-min}} / D_{98\%}$	Minimum dose to 98% volumes
$D_{\text{near-max}} / D_{98\%}$	Maximum dose to 2% volumes
$d_{10} / (10)_x$	10 cm depth technique
$\emptyset$	Diameter
TBq	Terabecquerel
mAs	Milliampere-seconds
$^{60}\text{Co}$	Cobalt-60 radioactive
$^{137}\text{Cs}$	Caesium-137 radioactive
NaI	Sodium Iodide
C	Coulomb (charge)
pA	Pico Ampere
nA	Nano Ampere
pC	Pico charge
$\text{Al}_2\text{O}_3:\text{C}$	Carbon-doped aluminum oxide polycrystal
eV	Electron volt
$D_{\text{max}}$	Maximum dose depth
$Z_{\text{max}}$	Maximum dose depth
J/kg	Joule per kilogram
$dE_{\text{tr}}$	Ionizing particles released by uncharged particles (photon)

$d_m$	Material mass
MeV	Mega electron volt
cGy	centiGray
K	Kerma
keV	Kilo electron volt
$\mu_{en}$	Energy absorption coefficient
$\mu_{tr}$	Energy transfer coefficient
$N_{D,w,Co}$	Mose to water calibration coefficient
Q	Beam quality
$k_{Q,Co}$	Calibration coefficient for another beam quality
Gy	Gray
$R^2$	Regression coefficient
$V_D$	Volume dose
$\rho_e$	Electron density
$\rho_m$	Mass density
$N_A$	Avogadro's number
$\chi^2$	Chi square test
$\mu$	Linear attenuation coefficient
$\mu/\rho$	Mass attenuation coefficient
$\rho_{tissue}$	Tissue density
$w_i$	Percentages by mass for each element of the respective tissue
$z_{ref}$	Reference depth
$N_{K,Co}$	Kerma in air calibration coefficient
$\mu Ci$	Microcurie
kVp	Kilovoltage peak
HU $\rho$	Hounsefield unit density
$\rho$	Density
MV	Megavoltage
MeV	Mega electron volt



## LIST OF ABBREVIATIONS

2D	2 dimensional
3DCRT	Three-Dimensional Conformal Radiotherapy Technique
3D	3 dimensional
AAPM	American Association of Physicists in Medicine
ABS	Acrylonitrile butadiene styrene
ANOVA	Analysis of variance
ASR	Age-standardized incidence rate
ASTRO	American Society for Radiation Oncology
AT	Anterior
AV	Axillary vessel
BC	Breast cancer
BMB	Brass mesh bolus
BEV	Beam's Eye View
BG	Background count
CB	Contralateral breast
CBCT	Cone beam computed tomography
CET	Coefficient equivalent thickness
CM	Composite material
CPM	Counts per minute
CT	Computed Tomography
CT-MD	Computed Tomography-Mass Density
CT-RED	Computed Tomography-Relative Electron Density
CTV	Clinical target volume
Df	Degrees of freedom
DFS	Disease Free Survival
DRR	Digital reconstructed radiographs
DVH	Dose Volume Histogram
EBCTOG	Early Breast Cancer Trialists' Collaborative Group
EBRT	External Beam Radiation Therapy
EBT3	Gafchromic EBT3 film
EDP	Electron Density Phantom

ED	Electron density
EPID	Electronic Portal Imaging Device
F	F value is used in analysis of variance (ANOVA). It is calculated by dividing two mean squares.
F-IMRT	Field in Field Intensity Modulated Radiation Therapy
FLUKA	FLUKA is a fully integrated particle physics MonteCarlo simulation package
FIF	Field in Field
FOV	Field of View
GATE	GATE a simulation platform for nuclear medicine based on GEANT4
GEANT 4	Geant4 is a platform for "the simulation of the passage of particles through matter
GE CT	GE Computed Tomography
GM	Geiger–Müller
GTV	Gross Tumor Volume
HI	Homogeneity Indec
HL	Hodgkin lymphoma
HU	Hounsefield Unit
HV	High Voltage
IAEA	International Atomic Energy Agency
IC	Ionization Chamber
ICRU	The International Commission on Radiation Units and Measurements
ICRP	International Commission on Radiological Protection
IEC 60731	Medical electrical equipment - Dosimeters with ionization chambers as used in radiotherapy
IGRT	Image-guided radiation therapy
IKN	Institut Kanser Negara
IM	Internal margin
IMN	Internal Mammary Nodes
I-IMRT	Inverse Intensity Modulated Radiation Therapy
IMRT	Intensity Modulated Radiation Therapy
IORT	Intraoperative radiation therapy
IP	Inter-pectroral nodes
IPPT	Institut Perubatan & Pergigian Termaju
ITV	Internal Target Volume
LAT	Lateral

Lt	Left
LED	Light-emitting diode
LINAC	Linear accelerator
LRR	Loco-regional recurrence
LRF	Locoregional failure
MC	Monte Carlo
MD	Mass density
MLC	Multi-leaf collimator
MONACO	Elekta's treatment planning system
MOSAIQ	A certified health information system that manages the treatment of cancer patients in both the medical oncology and radiation oncology healthcare setting.
MPV	Mean Pixel Value
MRI	Magnetic Resonance Imaging
MS	Mean sum of squares
NCAT	National Cancer Action Team
NCR	National Cancer Registry of Malaysia
NIST	National Institute of Standards and Technology USA
NRC	States Nuclear Regulatory Commission
NRIG	National Radiotherapy Implementation Group
NTCP	Normal Tissue Complication Probability
SI	International System of Units
SM	Setup margin
SSDL	Secondary Standard Dosimetry Lab
PACS	Picture archiving and communication system
Pm	Pectoralis minor
PHA	Polyhydroxyalkanoates
PLA	Polylactic Acid
PLD	Photoluminescent dosimeter
PM	Pectoralis Major
PSDL	Primary Standard Dosimeter Laboratory
OAR	Organ at risk
OS	Overall survival
OSLD	Optically stimulated luminescent dosimetry
PDD	Percentage Depth Dose

PMT	Photomultiplier tube
PRV	Planning Organ at Risk
PTV	Planning Target Volume
PTW-Unidos	Dosimeters used for measuring air kerma and absorbed dose to water.
PMRT	Post-Mastectomy Radiotherapy
QA	Quality Assurance
QC	Quality Control
QUANTEC	Quantitative Analysis of Normal Tissue Effects in the Clinic
RED	Relative Electron Density
RT	Radiation Therapy
Rt	Right
RTCW	Right Chest Wall
RTPS	Radiotherapy Treatment Planning System
ROI	Region of Interest
SCF	Supraclavicular field
SPV	Spot Placement Volume
START	The UK Standardization of Breast Radiotherapy
SS	Sum of squares
SSD	Source Surface Distance
T3	T3 tumor stage
T4	T4 tumor stage
T-test	Statistical analysis
TCP	Tumor Control Probability
TLD	Thermoluminescent dosimeter
TG-51	Task Group No. 051 - AAPM's Protocol for clinical reference dosimetry of high-energy photon and electron beams (1999)
TG-53	Task Group No. 053 – AAPM Quality assurance program for radiotherapy treatment planning
TG-66	Task Group No 083 - AAPM Quality assurance for computed-tomography simulators and the computed-tomography-simulation process
TG-132	Task Group No 132 – AAPM Use of Image Registration and Data Fusion Algorithms and Techniques in Radiotherapy Treatment Planning
TG-191	Task Group No. 191 - AAPM Recommendations on the Clinical Use of Luminescent Dosimeters
TRS-398	Technical Report Series-398 Absorbed Dose Determination in

	External Beam Radiotherapy: An International Code of Practice for Dosimetry based on Standards of Absorbed Dose to Water Universiti Sains Malaysia
USM	
VMAT	Volumetric Modulated Arc Therapy
WBRT	Whole Breast Radiotherapy
XCOM	Photon Cross Sections Database
XVI	X-Ray volumetric Imaging

## **LIST OF APPENDICES**

- Appendix A      Nanodot Readout Procedure
- Appendix B      Therapy Dosimeter Calibration Sheet
- Appendix C      Beam Summary Report Right Chest Wall Bolus
- Appendix D      Beam Summary Report Right Chest Wall Brass Mesh Bolus

**PENGESAHAN DOS BOLUS JEJARING LOYANG UNTUK  
PASCAMASTEKTOMI PAYUDARA KONTRALATERAL DALAM TEKNIK  
RADIOTERAPI KONFORMAL TIGA DIMENSI**

**ABSTRAK**

Rawatan radioterapi selepas mastektomi (PMRT) disarankan kepada pesakit yang menjalani pembedahan mastektomi payudara. Dengan penggunaan bolus dalam PMRT, ia telah menunjukkan beberapa had di mana bolus setara air semasa ini (WEB) tidak dapat merangkumi permukaan yang tidak rata dengan konsisten. Selain itu, ketidakaturan dos berlaku pada payudara kontralateral (CB) dan organ berisiko (OAR) semasa PMRT. Telah terbukti bahawa bolus jejaring tembaga (BMB) mempunyai potensi untuk merangkumi permukaan yang tidak rata dengan tujuan untuk merawat kawasan dinding dada dalam memberikan dos maksimum dan meminimalkan dos kepada OAR. Kajian ini bertujuan untuk menentukan kebolehlaksanaan BMB sebagai alternatif kepada bolus WEB dan untuk mengesahkan dos yang diterima oleh CB dan payudara sasaran dengan penggunaan BMB dalam terapi radiasi konformasi tiga dimensi (3DCRT). Kajian ini dilaksanakan berdasarkan tiga bahagian utama; pertama adalah untuk mengkalibrasi dosimeter (Ludlum, kebuk pengion dan nanoDot™) berdasarkan tenaga foton Cobalt-60 dan 6-MV; kedua adalah untuk mengukur sifat radiologi, fizikal dan dosimetri BMB dengan mengukur kepadatan menggunakan tiga metodologi (analisis Image-J, kepadatan konvensional dan analisis CT), pekali penyerapan jisim, pekali penyerapan tenaga jisim dan peratusan dos kedalaman (PDD); dan yang terakhir adalah untuk mengesahkan rawatan radioterapi dengan BMB kepada fantom heterogen PMRT dengan kaedah 3DCRT. Penilaian analisis statistik mengikut piawai antarabangsa telah dilaksanakan. Hasil kajian menunjukkan

bahawa semua dosimeter mempunyai lineariti yang tinggi dengan kebolehesanan yang boleh dijejaki. Untuk kajian sifat radiologi dan fizikal BMB; pertama, nilai kepadatan menunjukkan tiada perbezaan statistik antara tiga metodologi yang berbeza berdasarkan analisis varians (ANOVA); kedua, pekali penyerapan jisim menunjukkan perbezaan 1.1% antara analisis XCOM-Eksperimental dan XCOM-GATE; dan akhirnya, nilai pekali penyerapan tenaga jisim adalah selari dengan nilai yang diberikan dari XCOM tisu payudara dengan ralat 2.4 %. Sifat dosimetri BMB menunjukkan PDD yang lebih baik pada kedalaman 1 cm dan serapan dos yang tinggi pada kedalaman maksimum 6 MV foton iaitu pada 1.5 cm berbanding superflab. Ini boleh meningkatkan kesan penghindaran kulit kerana dos pembinaan dan dos permukaan yang lebih tinggi. Untuk bahagian ketiga, pelan dinding dada kanan dengan BMB mengandungi lengkungan dos 107% yang lebih besar dari dos perskripsi (4000 cGy) dalam isipadu sasaran perancangan (PTV) berbanding bolus superflab. Walaupun superflab mempunyai lengkungan dos 107% yang rendah, ia menyumbang kepada serapan dos yang lebih tinggi iaitu sebanyak 4500 cGy berbanding BMB. BMB mampu mengedarkan serapan dos 107% yang lebih rendah sepanjang PTV. Keputusan ini menunjukkan bahawa BMB adalah salah satu bolus yang boleh digunakan untuk PMRT.



# **DOSE VERIFICATION OF BRASS MESH BOLUS FOR CONTRALATERAL BREAST POST-MASTECTOMY IN THREE-DIMENSIONAL CONFORMAL RADIOTHERAPY TECHNIQUE**

## **ABSTRACT**

Post mastectomy radiation therapy (PMRT) prescribed to patient that undergo breast mastectomy. With the bolus application in PMRT, it has shown few limitations whereby current water equivalent bolus (WEB) unable to conform irregular surface consistently. Besides that, dose inhomogeneity arises in contralateral breast (CB) and organ at risk (OAR) during PMRT. It is established that brass mesh bolus (BMB) has potential in conforming irregular surface with the aim to treat chest wall site in delivering maximum dose and sparing OAR. This study aims to determine the feasibility of BMB as an alternative to bolus and to verify dose received by CB and target breast with application of BMB in 3-dimensional conformal radiation therapy (3DCRT). This study are designed based on three main parts ; firstly is to characterize dosimeters (Ludlum detector, ionization chamber and nanoDot<sup>TM</sup>) based on Cobalt-60 and 6-MV photon energy; secondly is to measure the radiological, physical and dosimetric properties of BMB by measuring the density using three methodologies (Image-J analysis, conventional density and CT analysis), mass attenuation coefficient, mass energy absorption coefficient and percentage depth dose (PDD) ; and lastly is to verify the radiotherapy treatment with the BMB to the PMRT heterogenous phantom by 3DCRT. Statistical analysis evaluation in accordance with the international standard was applied. The results revealed that all dosimeters have high linearity with acceptable traceability. For the radiological and physical properties of BMB study; firstly, the density values indicate no statistical difference between three

different methodologies based on analysis of variance (ANOVA); secondly, the mass attenuation coefficient shows 1.1% differences between analysis of XCOM-Experimental and XCOM-GATE; and lastly the mass-energy absorption coefficient value was in good agreement with the given value from XCOM of breast tissue with 2.4% error. The dosimetric properties of BMB indicates superior PDD at depth 1 cm and comparatively high at maximum depth of 6 MV photon (1.5 cm) contrasted to superflab. This may increase the skin sparing effect as the build-up dose and surface dose is higher. For the third part, the right chest wall plan with BMB contained larger 107% isodose curve from the prescription dose (4000 cGy) within the planning target volume (PTV) compared to Superflab bolus. Even though, superflab bolus display a lower region of 107%, however it accounts for higher absorbed dose which is 4500 cGy. BMB able to distribute low 107% dose along the PTV compared to superflab. These results shows that BMB is one of the probable boluses to be applied in PMRT.

# CHAPTER 1

## INTRODUCTION

### 1.1 Background of Study

Female breast cancer is the first common cancer case in Malaysia, where 32.1% of cases are in women. 21,925 new cases of breast cancer were recorded from 2012 to 2016 by the National Cancer Registry of Malaysia (NCR), with an age-standardized incidence rate (ASR) of 34.1 per 100,000 women (National Cancer Registry, 2016). With the number of female breast cancer cases is gradually increasing, the therapy plan for breast cancer shall be reviewed regularly to increase the rate of patient survival rates. Generally, most of the breast cancer cases were treated with mastectomy surgery (Barrett et al., 2009). Following a mastectomy, the main course of treatment for breast cancer patients is post-mastectomy radiation therapy (PMRT). PMRT increases locoregional control and overall patient survival rates (Remick & Amin, 2020). PMRT is irradiation directly to the chest wall by combining 4 to 5 irradiation techniques that are recommended to patients with specific conditions. The conditions are ; the patient was diagnosed with tumor bigger than 5 cm across (T3) and tumor has spread into chest wall (T4) ; patient with four or more positive axillary nodes ; and patient that have high risk of local recurrence with more advanced disease with high-risk pathological characteristics (Gao et al., 2003).

68% of oncologist prefer bolus application in PMRT (Wong, Lam, Bosnic, et al., 2020). Bolus is a tissue equivalent material explicitly put on the skin surface to regularize the distribution forms as a flat surface typical to the beam (Vyas et al., 2013). Bolus is broadly utilized in PMRT to supply adequate dosage build-up within the skin and anterior part of the chest wall (Andic et al., 2009; Thoms et al., 1989) The response of the bolus on the skin surface is advantageous in PMRT, where brisk

erythema is accomplished (Su et al., 2014). Commercially accessible bolus materials widely used in radiotherapy are Superflab and Vaseline based boluses. These boluses, however, has several drawbacks. The most reported drawbacks are that these types of boluses unable to adhere completely to the treatment area and produce large air gaps (Chung et al., 2012). This is due to the irregular surface of chest wall and limited flexibility of these boluses. Air gap existed may consequently affect the PMRT course. It has been reported that air gaps up to 10 mm may cause a 10% drop in surface dose (Vyas et al., 2013). According to another study, the patient would suffer from hotspots and cold patches in the dose area if there was an air gap between the patient's skin and the bolus(Lobo et al., 2021). Another drawback of tissue equivalent bolus is that it is necessitates for two treatment plans: one for bolus and the other for no bolus. This could result in discrepancies in attenuation between the presence and absence of a bolus, which could lead to additional dose treatment errors (Butson et al., 2000).

It is established that brass mesh bolus (BMB) has substantial potential in striking the balance between the main objective of PMRT to treat the target site in delivering maximum dose to the chest wall and minimizing dose to organ at risk (OAR). The viability of BMB as a breast radiotherapy bolus had been investigated by a number of organisations in several nations including the United States, the United Kingdom, California, Australia, Korea, and Chicago (Al-Rahbi et al., 2018; Fiedler et al., 2021; Healy et al., 2013; Manger et al., 2016; Richmond et al., 2016). Brass mesh has been successfully implemented as a substitute to tissue-equivalent bolus in international institutions, i.e. University of California Davis Medical Centre in breast and head and neck cases (Healy et al., 2013). One of the findings of BMB application is the skin dose effects of PMRT were reported by Healy et al. study where moderate erythema (grade 2) was achieved in most patients (Healy et al., 2013). Another finding

claimed by Ordonez et al, study is that when using BMB as opposed to a tissue equivalent bolus the effect on percentage depth dose (PDD) can be reduce (Ordonez-Sanz et al., 2014). When compared to a water equivalent bolus, Al-Rahbi et al, claimed that the BMB has the strongest advantages that show its capacity to conform to the patient's surface with few air spaces and achieve uniform dosage distribution (Al-Rahbi et al., 2018). These significant reported advantages of BMB have contributes to possible alternatives of bolus application in reducing the drawbacks arise in PMRT.

Considering these BMB advantages in PMRT, to investigate the BMB for contralateral breast (CB) PMRT associate with three-dimensional conformal radiotherapy technique, the study design was designed by reviewing the radiological and dosimetric properties of BMB and verifying the dose delivered to the target site which is maximum dose to the chest wall and sparing the organ at risk (OAR).

## **1.2 Problem Statement**

Two problem statements have been outlined in this research. The first problem statement is the commercially Superflab, Vaseline based bolus and tissue equivalent bolus shows limitation on conforming irregular surface. In current radiotherapy practices, tissue equivalent boluses like Superflab, Vaseline, and wet boluses are frequently utilized as a bolus application (Andic et al., 2009; Hsu et al., 2008; Sroka et al., 2010). Studies have shown obstacles in the usage of water equivalent bolus whereby conformity to the chest wall was almost not achieved (Y. Khan et al., 2013). The inflexible structure of these types of boluses gives disadvantages in lowering the build-up dose at the target site and commencing the air gaps between the bolus and target (Sroka et al., 2010). Unnecessary air gaps occurred may subsequently affect the post mastectomy radiation therapy (PMRT) course as it has been reported that air gaps

up to 10 mm may cause a 10% drop in surface dose (Vyas et al., 2013). Such effects may significantly reduce the delivery of maximum dose to the target site in PMRT. Brass mesh bolus (BMB) has been shown to be a successful bolus for PMRT treatment. However, its feasibility in Malaysia has not yet been investigated as most of the PMRT practices in Malaysia utilized water equivalent bolus. The information of current PMRT practices with bolus has been gathered by qualitative interviews from several private and national radiotherapy center in Malaysia. To the best of the author's knowledge, there was almost none radiological and physical data of BMB as a tissue-equivalent bolus in radiotherapy application. With the current gap arises, this research aims to determine the BMB feasibility in physical and radiological aspects as potential bolus application in PMRT.

The second problem statement presented is the dose inhomogeneity arises in contralateral (CB) and organ at risk (OAR) during PMRT. Several consequences related to dose inhomogeneity during PMRT has been reported. Toxicity induction such as fibrosis, erythema, moist desquamation, and oedema may occur if dose inhomogeneity to the treated breast arises in radiotherapy (Tortorelli et al., 2013). Besides to pulmonary complications, an increasing difficulty has been tended to cardiovascular mortality recognized with left-sided complete breast irradiation (Darby et al., 2011). As for traditional tangential field-in-field, dose inhomogeneity is frequently cannot be avoid especially for large breast patients (Veldeman et al., 2016). There are no recommendations on protected dose ranges to the heart in three-dimensional conformal radiation therapy (3DCRT) technique application. Protocol as ICRU 83 for protected dose ranges to OAR available for Intensity Modulated Radiation Therapy (IMRT) (ICRU 83,2010). Compromising both OAR and target volumes in PMRT remains as one of the most major challenges in reducing dose

inhomogeneity. From literature reviews conducted, it has indicated that there was no extensive study to validate the dose heterogeneity arises in the contralateral breast and organ at risk during PMRT with BMB. Therefore, this research aims to verify dose received by OAR with BMB application to further improve the dose inhomogeneity occur in PMRT.

### **1.3 Research Objectives**

The research aim following to specific objectives is distinctly described as follows. The aim of this research is to determine the feasibility of brass mesh bolus (BMB) as one of the alternative bolus applications under megavoltage photon irradiation, for post-mastectomy radiation therapy (PMRT).

The verification of dose received by organ at risk (OAR) and contralateral breast (CB) with respect to BMB application is anticipated to be accomplished. The results of this study were anticipated to prominently enhance current clinical practices with a solid new methodology, as well as to significantly improve the quality of PMRT in local Malaysian hospitals by offering an alternate type of bolus. This research was conducted based on three specific objectives which are:

1. To determine the radiological and dosimetric properties of BMB as an alternative tissue-equivalent bolus.
2. To characterize the suitable dosimeter for BMB dose verification in PMRT to a justifiable calibration traceability.
3. To validate the dose received by contralateral breast (CB) and target breast with BMB in tangential 3DCRT.

#### **1.4 Research Significance**

This research will provide new insights into the brass mesh bolus (BMB) application in clinical procedures of post-mastectomy radiation therapy (PMRT). Through this research, a thorough radiological, physical and dosimetry information will further reveal the BMB advantages for future PMRT application. Medical institutions may also consider BMB as an alternate bolus type against current water-equivalent bolus. Moreover, the analysis presented in this study will convey valuable information for future research exploring the BMB benefits with the latest radiotherapy technique.

#### **1.5 Scope and Limitation of the Research**

The scope of this study consists of three major parts specifically. Part one is the radiation dosimeter analysis, whereby part two is the brass mesh bolus (BMB) properties evaluation. Part three is the application of BMB in post-mastectomy radiation therapy (PMRT). In part one, characterization of dosimeter in corresponding to Cobalt-60 energy with dosimeters (Ludlum Gieger Muller (GM) detector, NanoDot™ and Ionization chamber) were conducted. Characterization of dosimeter in corresponding to megavoltage (MV) energy for NanoDot™ and Ionization chamber dosimeter type were performed. In part two, BMB properties evaluation in terms of radiological, physical and dosimetry were presented. Whereas in part three, this section includes preparing a sample of the bolus, i.e., standard, and brass mesh bolus, phantom simulation under computed tomography (CT) simulator according to standard chest scan protocol, treatment planning, irradiation of phantom to mastectomy side, and dose evaluation, i.e., mastectomy side and contralateral breast (CB) side. This study will determine the dosimetry properties of BMB as bolus function and radiotherapy parameters during a PMRT course where total mastectomy of the breast has been



conducted. This will be represented by a right mastectomy phantom build up from layers of perspex.

The limitation of the study is distinctly stated as follows. The first limitation of this studies is this research only focuses to the exposure and irradiation of radioactive sources and photon to BMB at 1.25 MeV and 6 MV. Second limitation of this study is the safety implication and thermal neutron production associated to higher photon energy is not covered.

## **1.6 Outline of thesis**

The thesis is organized into five chapters. Chapter 1 begins with an introduction to the background of the study. It then describes the specific research objectives, research questions and significance of the study. Chapter 2 presents a literature review that connects the current practice of the post-mastectomy radiation therapy (PMRT) course, the application of tissue-equivalent bolus with the problem that arises, and the further related theoretical terms to the new proposed methodology. Chapter 3 describes the research design and methodology used to investigate research objectives. It outlines the study's design, data collection process and data analysis approach. Chapter 4 reports the empirical results of the study. It discusses the data in all parts of the studies. The data analysis begins with the dosimeter evaluation follows by radiological, physical and dosimetric study and ends with dose evaluation from treatment planning system (TPS), together with evaluation of dosimeter applied to the phantom to verify the amount of dose received accordingly. Chapter 5 concludes the thesis by discussing the research results and provides recommendations to further improve PMRT and brass mesh bolus (BMB) bolus application impact.

## **CHAPTER 2**

### **LITERATURE REVIEW**

#### **2.1 Post-Mastectomy Radiotherapy (PMRT)**

##### **2.1.1 Anatomy of Breast**

Breast cancer can commence in different parts of the breast. A breast is made up of three main parts: lobules, ducts, and connective tissue. Most breast cancers begin in the ducts or lobules. Breast cancer spreads locally to underlying muscle and overlying skin, including nipple through direct infiltration from lymph nodes (Barrett et al., 2009). The breast is located over the pectoralis major muscle on the anterior thoracic wall (Goethals & Rose, 2022). The breast is a symmetrical organ that can be seen either side of the midline on the front of the chest. It takes up space between the third and seventh ribs, as well as from the sternum's border to the armpit (Sandoz et al., 2013). In relation to numerous aspects including age, gland development, amount of fat, and relative influence of hormone stimulation, the volume, shape, and degree of the breast development are highly diverse (De Benedetto et al., 2016). The division of the breast into four quadrants enables uniform reporting of results from physical examinations or breast imaging. Upper inner, upper outer, lower inner, and lower outer are the four quadrants (Siotos et al., 2018).

In this paragraph, lymphatic drainage which is a part of breast anatomy was reviewed. Lymphatics flow superiorly to the supraclavicular fossa, medially to the internal mammary nodes, and laterally to the axilla. Lymphatic drainage is characterized to three levels as guidance for surgical axillary node dissection. All the breast's lymphatic arteries drain to the internal mammary nodes, which connect to the superior contralateral chain. Figure 2.1 (a-b) presents the level of lymphatic nodes in breast tissue

(Barrett et al., 2009). The external mammary, axillary vein, and scapular lymph node groups are among the Level I lymph nodes, which are those that are lateral to or beneath the lower border of the pectoralis minor muscle. As level II lymph nodes, the central lymph node group and possibly a few subclavicular nodes are positioned close to the pectoralis minor muscle. The level III axillary nodes, which are medial or superior to the top border of the pectoralis minor muscle, include the subclavicular lymph nodes (Goethals & Rose, 2022). Despite the complexity of the anatomical drainage arrangement, axillary lymph nodes are most frequently affected by tumor involvement.

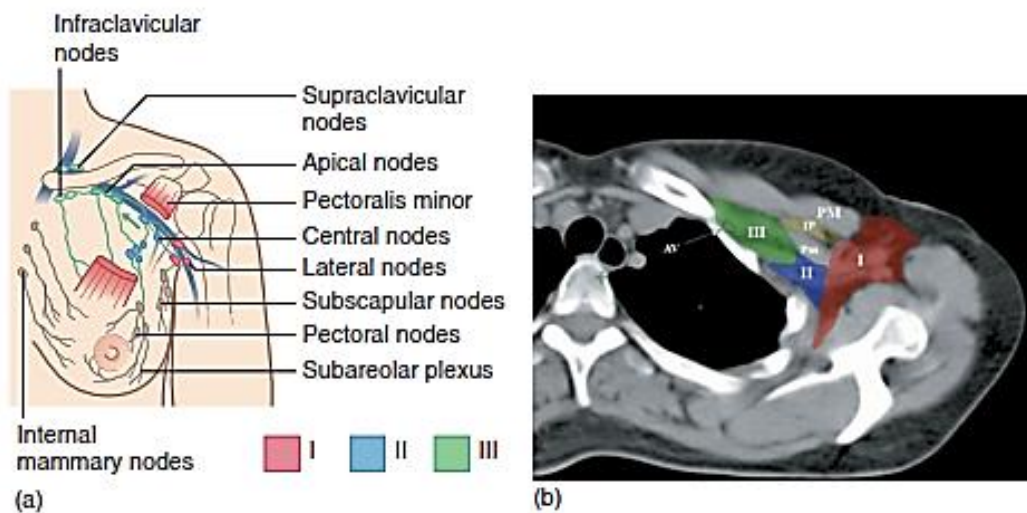


Figure 2.1: a) Lymphatic drainage of breast diagram. b) CT images in transverse plan of left breast with lymph nodes position. AV, axillary vessels; Pm, pectoralis minor; PM, pectoralis major; IP, inter-pectoral nodes (Barrett et al., 2009).

Mastectomy is a surgical surgery in which all or a portion of the breast is removed. A cancer of the breast is the most common reason for a mastectomy. Localized surgical treatment is typically required as the primary method of treating breast cancer (either mastectomy or breast-conserving surgery). The basis of breast cancer treatment is typically targeted surgery (either mastectomy or breast-conserving

surgery), which may be combined with neoadjuvant or adjuvant therapy such as radiation, chemotherapy, hormone antagonist drugs, or both (Goethals & Rose, 2022).

Along with our research interest, which was to improve the post-mastectomy radiation therapy (PMRT) course, a considerable amount of literature that has published on breast mastectomy benefits has been presented. After surgical resection, PMRT tries to eliminate any potential occult disease inside the chest wall components, which include the remaining breast glandular tissue, epidermis, subcutaneous lymphatic plexus, and local lymphatics (Abdulkarim et al., 2011; McGale et al., 2014). Numerous studies have shown that PMRT enhanced disease-free survival (DFS), overall survival (OS) and locoregional recurrence (LRR) (Abdulkarim et al., 2011; Boulle et al., 2019; Buchanan et al., 2006) The above finding on PMRT benefits is consistent with the previous study by Ragaz et al., in year 2005 (Ragaz et al., 2005). It has also been reported that women with affected axillary lymph nodes have been demonstrated to experience a four times reduction in LRR with PMRT, and all patient groups experience a decrease in breast cancer mortality (McGale et al., 2014). Based on the advantages of PMRT reported, it was evidence that PMRT is crucial in overall breast cancer therapy treatment.

### **2.1.2 PMRT Treatment Indication, Prescription and Radiotherapy Techniques**

Indication for PMRT treatment are for individuals with four or more positive lymph nodes, patients with (T3), T4 tumors with high risk of local recurrence (Tseng et al., 2015). Research findings by Frasier also point towards this (Frasier et al., 2016). T3 and T4 are based on tumor, nodes, and metastasis (TNM) staging where T3 was defined as cancer cells more than 5 cm whereby T4 were categorized into four groups. Four groups

comprise T4. T4a indicates that the malignancy has entered the chest wall. T4b indicates that the cancer has progressed to the skin and may be accompanied with breast swelling. T4c denotes that the cancer has progressed to the chest wall and the skin. Inflammatory cancer is denoted by T4d. This rare form of breast cancer is uncommon (Barrett et al., 2009). In 2014, the Early Breast Cancer Trialists' Collaborative Group (EBCTCG) published an updated meta-analysis of the effects of PMRT. According to this meta-analysis, there were no differences in breast cancer mortality or any first recurrence between the benefits of PMRT for individuals with a single positive node compared to those with two or three positive nodes (McGale et al., 2014). In a recent ASTRO guideline, the panel came to the unanimous conclusion that PMRT reduces the risk of locoregional failure (LRF), any recurrence, and breast cancer death for patients with T1 (tumors less than 2 cm) and T2 (cancer is more than 2 cm but no more than 5 cm) and one to three positive axillary nodes (Koh & Kim, 2022; Recht et al., 2016).

PMRT prescription were based on dose fractionation in absorbed dose (Gy). The dose fractionation to the chest wall were defined as several fractionation. The first fractionation is 40 Gy in 15 daily fractions with 2.67 Gy in three weeks. Second fractionation is 42.5 Gy in 16 daily fractions of 2.66 Gy in 3 ½ weeks and the third fractionation is 50 Gy in 25 daily fractions given in 5 weeks (Barrett et al., 2009). All these regimens have undergone successful START Trial A and B randomized trials testing (Agrawal et al., 2008). Fractionation 50 Gy in 25 daily fractions is the conventional radiation dose for PMRT (Chitapanarux et al., 2019). Fractionation as first and second are the standard hypofractionation prescriptions for PMRT. These hypofractionation regimens in PMRT have been investigated by several retrospective studies with promising outcomes (Bochenek-Cibor et al., 2020; Ko et al., 2015). Review

of PMRT indication and treatment prescriptions provide an important insight into the worldwide current practices and research focus in PMRT.

Radiation therapy techniques revolve from two dimensional, three dimensional and latest to intensity modulated techniques over the past decades. Research in PMRT has emphasized and continuously researching on the best techniques with balance dose distribution on target volume and organ at risk (OAR). Recent research comparing three-dimensional conformal radiation therapy (3DCRT) and intensity modulated radiation therapy (IMRT) procedures for left breast radiotherapy shows a significant improvement in left breast cancer conformity of plan, lower mean dosage, and lower high-dose volumes of the ipsilateral heart and lung in IMRT, although 3DCRT superior in terms of low-dose volume to OAR (Adeneye et al., 2021). This finding is consistent with findings of past studies by Rastogi et al. (Rastogi et al., 2018). In contrast, Wang et al, have reported that after a modified radical mastectomy, the mean accidental dose to the Internal Mammary Nodes (IMN) for Field in Field (F-IMRT) and Inverse (I-IMRT) and 3DCRT was insufficient to treat subclinical illness (Wang et al., 2019).. For 3DCRT and IMRT, larger accidental doses to the IMN were linked to higher heart mean doses and higher lung doses (Wang et al., 2019). In summary, several literatures have reported the benefits of IMRT technique in providing conformity to the target volume in PMRT, whereby 3DCRT technique able to retain low dose to OAR indicating the potential in sparing the OAR can be attained in PMRT.

### **2.1.3 Dosimetry Planning (Tissue Inhomogeneity Correction) and Three-Dimensional Conformal Radiation Therapy (3DCRT) Treatment Planning**

Applications of common isodose diagrams and depth dose tables presuppose a uniformly dense medium. This is condition is not always ideal as in patient there are

many layers where the beam transverse the respective compounds i.e. (fat, bone, muscle, lung, and air). Any inhomogeneity will induce changes in the dose distribution which depends on the type of material exist and the quality of beam radiation. Introducing new material across the beam path, inhomogeneity correction shall be complied (F. M. Khan & Gibbons, 2014). Khan and Gibbons documented few methods in correcting beam attenuation and scattering namely: a) tissue-air ratio method, b) power law tissue-air ratio method, c) equivalent tissue-air ratio method, d) isodose shift method and e) typical correction factor.

As reported in AAPM report no 85, there is a critical need for inhomogeneity corrections to achieved dose accuracy. In addition to that, AAPM report 85, the specific objectives were including a) review the clinical need for inhomogeneity correction b) review current available methodologies for tissue inhomogeneity correction in photon beams c) assessing the advantages and disadvantages of (b) and d) recommendations on the use of inhomogeneity correction in the clinical environment (AAPM 85,2004). Particularly with the introduction of 3D precision conformal radiotherapy and the expansion of intensity-modulated radiation therapy (IMRT) treatments to structures that have not previously been exposed to radiation, accurate dose determination, including inhomogeneity corrections, is a crucial component of dose optimization and the objective analysis of clinical results (Papanikolaou et al., 2004). There is a large volume of published studies describing the needs of tissue inhomogeneity corrections in breast and post-mastectomy radiation therapy. Preliminary work on the inhomogeneity correction application in tangential breast irradiation by Mijnheer et al, has been reported (Mijnheer et al., 1991). In the study, the authors reported that there is increase in dose in a high dose region by actual and in vivo measurement and recommended for inhomogeneity correctios for tangential breast irradiation. This is due to the inclusion

of lung tissue in the treatment volume which resulting in some parts of breast will receive higher dose (Mijnheer et al., 1991). In a study by Petillion et al, which set out to assess radiobiological impact of whole breast radiation therapy (WBRT) algorithm without correction of tissue inhomogeneity has reported that ignoring the inhomogeneity has arisen to radiobiological and clinical impact (Petillion et al., 2014). Apart from breast radiotherapy, inhomogeneity correction in the context of CT scanning is discussed in the study by Das et al, in year 2016 (Das et al., 2016). The demands for inhomogeneity tissue correction are crucial in the setting of radiotherapy especially in IMRT.

Three-dimensional conformal radiotherapy (3DCRT), treatments are based on 3D anatomic information and use treatment fields that conform as closely as possible to the target volume in order to deliver adequate dose to the tumor and minimum possible dose to normal tissue. Additionally, the idea of conformal dose distribution has been expanded to encompass clinical goals including increasing tumour control probability (TCP) and reducing the likelihood of complications with normal tissue (NTCP). 3DCRT technique encompasses both the physical and biologic rationales in achieving the desired clinical results. analytic plan recommended by the International Commission on Radiation Units and Measurements (Lanberg et al., 2016). In Ann Barrett et al, 3DCRT links the 3D CT images of the tumor with the capability of LINAC to design the beam geometrically and based on the final agreed PTV by oncologist and physicist. Basic 3DCRT consist of coplanar and static beams with multi-leaf collimator (MLC) to shape the volume (Barrett et al., 2009).

The main difference between the treatment planning of 3DCRT and conventional radiotherapy is that this technique requires the availability of 3D anatomic and system that is capable to calculating the 3D dose distribution. The treatment



planning process of 3DCRT technique consists of following points : i) imaging data by CT or MRI images, ii) image registration, iii) image segmentation, iv) beam aperture design, v) field multiplicity and collimation and vi) plan optimization and evaluation. (F. M. Khan & Gibbons, 2014).

#### **2.1.4 Bolus**

Bolus is an added tissue that introduces to the surface of the treated area with the advantages to imitate tissues by using materials approximately near to water or muscle to achieve dosimetric properties (Vyas et al., 2013). Bolus was introduced with the aim of reducing skin sparing effect of megavoltage photons and to achieve flat isodose lines of irregular patient surfaces. Other purpose of bolus is to ensure that the chest wall receives an adequate dose and increase the dose to the skin surface (Wong, Lam, Bosnic, et al., 2020). Bolus material can be used to alter the depth of the maximum radiation dose ( $D_{max}$ ) during radiation therapy (Sroka et al., 2010).

Vu et al. observed that 68% of radiation oncologists utilised bolus frequently, 6% never, and 26% depending on the situation for PMRT in their study of 1035 radiation oncologists from the Americas, Europe, Australia, and Asia (Vu et al., 2007). Substantial numbers of disadvantages in standard bolus application have been reported. The reviewed literature suggests that there are limitations as Khan et al. found that employing orthogonal static 6 MV beams and radiation fields smaller than  $10 \times 10 \text{ cm}^2$ , air gaps bigger than 1 cm under the bolus result in a dose reduction at surface of more than 10% (Y. Khan et al., 2013). Butson et al. and Chung et al. have found similar findings, with the greatest notable dose decreases when taking angles of radiation incidence closest to the perpendicular direction and smaller fields into account (Butson et al., 2000; Chung et al., 2012). This may induce unnecessary underdose cases to the target.

Literature on the advantages of the bolus application were gathered from multiple research studies. A recent study by Kawamoto defined that tissue-equivalent materials are applied to the chest wall to provide dose build-up in the skin and tissue in order to adequately deliver the prescription dose to the level of skin and treat residual disease (Kawamoto et al., 2021). This was demonstrated by Yoon et al. work which used an anthropomorphic phantom to evaluate skin dose and discovered that a 1-cm superflab bolus has boosted the dose at the chest wall and skin, ensuring that these locations received doses more than the recommended amount (Yoon et al., 2018). Besides that, previous study has reported that the bolus helps the radiation penetrate deeper into the epidermis to deliver the required dose (Sroka et al., 2010).

Apart from that, a study involving breast cancer patients who received adjuvant radiation to the chest wall with bolus application, a lower risk of chest wall recurrence was associated with increased skin erythema, which is likely a sign of a higher skin dose (Fiedler et al., 2021). Besides that, the thickness of the bolus and subcutaneous tissue influence the movement of the 95% isodose line closer to the skin and subcutaneous tissue which according with the PMRT objective (Dahn et al., 2021). With this majority of oncologists utilized the bolus application and promising advantages listed in previous discussion, the needs of bolus application improvement demand to be addressed.

#### **2.1.4(a) Bolus Material**

With the complexity of radiation treatment, substantial studies in developing bolus material have been conducted in line with the requirement and advancement of radiotherapy treatment. The bolus material can be a soft, rubbery tissue equivalent material placed in direct contact with the patient's skin surface. Table 2.1 below summarizes the findings of bolus material development throughout the literature review.

Table 2.1: Literature review summary of brass material

Author, Year	Type of bolus material	Bolus material
Boman et al., 2018; J.A Diaz-Merchan et al., 2022	Water-equivalent material Water-equivalent material	1. Paraffins 1. Bolus CM - Made up of organic compounds and glycerol 2. Acrylonitrile Butadiene Styrene (ABS) plastic 3. PLA plastic 4. Constructed of silicone rubber formed from 3D printed casts.
Boulle et al., 2019	Water-equivalent material	1. Custom silicone 0-1 cm
Eric et al., 2020	Water-equivalent material	1. Copper and copolymer– Polylactic Acid (PLA) 2. Polyhydroxyalkanoate (PHA)-plastic composite material Manufacturer: Copperfill, ColorFabb, Venlo Netherlands
Apipunyasopon et al., 2020	Water-equivalent material	1. Superflab4 Manufacturer: Radiation Products Design Inc, Albertville, MN
Chiu et al., 2018 Manger et al., 2016	Water-equivalent material Water-equivalent material	1. Organic polymer compounds, 1. Flab-like gel-based products rubber
Nagata et al., 2012	Water-equivalent material	1. Wax 2. Play doh
Sazirul et al., 2020	Water-equivalent material	1. Beeswax
Vyas et al., 2013	Water-equivalent material	1. Polymer gel
Asher et al., 2017	Tissue-equivalent material	1. Brass Mesh Bolus, 50cm x 50cm Manufacturer: Radiation Products Design Inc, Albertville, MN
Al Sudani et al., 2020	Tissue-equivalent material	1. eXaSkin Manufacturer: Anatomical Geometry S.L.
Lobo et al., 2021	Tissue-equivalent material	1. Brass Mesh Bolus, 50cm x 50cm Manufacturer: Radiation Products Design Inc, Albertville, MN

Fiedler et al., 2021	Tissue-equivalent material Water-equivalent material	1. Brass Mesh Bolus, 50cm x 50cm Manufacturer: Radiation Products Design Inc, Albertville, MN 2. Polymer-gel bolus
----------------------	---------------------------------------------------------	--------------------------------------------------------------------------------------------------------------------------

#### **2.1.4(b) Bolus Technique**

Recently in clinical radiotherapy practices, there are many techniques in applying and producing bolus to the patient. Bolus techniques have been reported in several publications in enhancing the radiotherapy (Boman et al., 2018; Opp et al., 2013; Tyrann et al., 2018) Generally, bolus techniques can be divided into four categories which are three-dimensional (3D) printing, planar commercial bolus, virtual bolus and planar varying thickness bolus. 3D printing is a technique that precisely matches the patient surface contour. Planar commercial is a traditionally, water-/tissue-density equivalent or molded wax that was positioned over the treatment region (Dyer et al., 2020). Whereas virtual bolus is a technique which creating a treatment plan using a virtual bolus generated by the software (Rafli et al., 2021).

#### **2.1.5 Plan Dose Evaluation**

Conventionally, 3DCRT plan dose evaluation consists of reviewing isodose curves, surfaces curves and dose volume histograms. Other aspects as discussed below have been incorporated from other radiotherapy treatment technique, IMRT to critically review the plan.

##### **2.1.5(a) Dose Coverage of Planning Target Volume (PTV) and Organ at Risk (OAR)**

Different target volumes (such as GTV, CTV, and PTV) should be carefully developed while taking into account any inherent constraints or uncertainties at each stage of the

procedure (F. M. Khan & Gibbons, 2014). Target Volumes in Radiation Oncology have been classified into Gross Tumor Volume (GTV), Clinical Target Volume, Irradiated Volume (IV), Planning Target Volume (PTV), Organ at Risk (OAR) and Planning Organ at Risk (PRV). There is extension of volumes and margin definition from ICRU 50 to ICRU 62 where PRV, Internal margin (IM), Setup margin (SM) and Internal Target Volume (ITV) were introduced (Lanberg et al., 2016) (International Commission on Radiation Units and Measurements, 1999). Each definition of the volumes and margin was presented in Table 2.2 below.

Table 2.2: Definition of volume in accordance with ICRU 50 and 62.

Volume	ICRU	Definition
GTV	50	<b>Gross Tumor Volume</b> - Gross palpable or visible demonstrable extent and location of cancer growth
CTV	50	<b>Clinical Target Volume</b> - Tissue volume that contains GTV and/or subclinical microscopic cancer disease which need to be eliminated and adequately treated to achieve aim of therapy - For external beam therapy (EBRT) margin added around CTV to compensate effects of organ movement and patient set up
PTV	50	<b>Planning Target Volume</b> - Geometrical definition and defined to choose appropriate beam and arrangements. - To ensure prescribed dose absorbed by CTV
TV	50	<b>Treated Volume</b> - Volume enclosed by isodose surface, selected, and specified by oncologist to achieve the eradication of tumor
IV	50	<b>Irradiated Volume</b> - Tissue volume which receives dose that is significant to normal tissue tolerance
OAR	50	<b>Organ at Risk</b> - Normal tissue which the radiation sensitivity may influence treatment planning and/or prescribed dose
IM	62	<b>Internal Margin</b> - Margin that must added to CTV to compensate for expected movement and variations in size, shape, and position of CTV during therapy

ITV	62	<b>Internal Target Volume</b> <ul style="list-style-type: none"> <li>- Represent the volume enclosing the CTV and internal margin</li> <li>- Related to patient coordinate system</li> </ul>
SM	62	<b>Set-up Margin</b> <ul style="list-style-type: none"> <li>- To account for uncertainties associated by inaccuracies and lack of reproducibility in patient positioning and alignment of therapeutic beam.</li> <li>- Referenced in the external coordinate system</li> </ul>
PRV	62	<b>Planning Organ at Risk Volume</b> <ul style="list-style-type: none"> <li>- Integrated margin added to OAR to compensate for uncertainties.</li> <li>- Including size of the combined margin of OAR in different directions.</li> <li>- PTV and PRV may intersect</li> </ul>

In dose coverage of PTV and OAR, the isodose curves encompassed the PTV and OAR was reviewed. The ICRU had previously advised that the PTV's absorbed dose be limited to between 95% and 107% of the recommended absorbed dose (International Commission on Radiation Units and Measurements, 1999). One can evaluate the dose distributions of competing methods by looking at isodose curves in individual slices, orthogonal planes (such transverse, sagittal, and coronal), or 3-D isodose surfaces. One of the key advantages of 3-D treatment planning is the capability to change the dose distribution presentation to show volumetric dose coverage as individual slices, in orthogonal planes, or as 3-D isodose surfaces (F. M. Khan & Gibbons, 2014). When the dosage distribution is normalized to 100% at the time of dose prescription, the isodose curves indicate lines of equal dose expressed as a percentage of the prescribed dose. (Lanberg et al., 2016).

Because an OAR's absorbed-dose distributions are non-homogeneous, it has been customary to employ the idea of dose-volume reporting stating  $V_D$ , which is a volume that gets at least the absorbed dose  $D$ , for OAR reporting when using the IMRT technology (Menzel, 2010). For instance, Pan et al, discovered that  $V_{20\text{ Gy}}$ , the volume

of normal lung receiving more than 20 Gy, was well linked with the incidence and severity of lung pneumonitis (Pan et al., 2017) where lung served as OAR in breast radiotherapy, hence details consideration for sparing lung should be critically reviewed. Tang et al, in their research on five advanced PMRT techniques by IMRT with SIB for the left breast cancer patients have evaluated and compared in terms of target coverage dose and dose sparing of OARs (Tang et al., 2020). Hence reporting  $V_D$  for high-risk OAR is crucial in IMRT technique and can be applied for other treatment technique such as 3DCRT for critically evaluate the respective plan.

### **2.1.5(b) Dose Volume Histogram (DVH)**

Isodose curves or surfaces are useful for displaying the dose distribution because they highlight the anatomical location and size of uniform, high, or low dose zones. In addition to DVHs for the segmented structures, such as targets and critical structures, this information is essential for 3-D treatment planning. A DVH not only integrates the complete dose distribution into a single curve for each anatomic structure of interest, but also offers quantitative data on how much dosage is absorbed in how much volume. As a result, it is an excellent tool for evaluating a particular strategy or comparing opposing viewpoints (F. M. Khan & Gibbons, 2014).

The cumulative integral DVH and the differential DVH are the two ways the DVH can be represented. A representation of the volume of a particular structure getting a specific dose or more as a function of dose is called the cumulative DVH. The volume that achieves the prescribed dose or greater is shown on the cumulative DVH curve at any point. A volume plot is represented by the differential DVH. getting a dosage in accordance with a dose at a set dose interval (Pyakuryal et al., 2010). The cumulative DVH has been found to be more useful and is more prominently used than the differential form (F. M. Khan & Gibbons, 2014).

### 2.1.5(c) Homogeneity Index (HI)

The characteristics of the quality of the absorbed dose distribution are dosage homogeneity and dose conformance, which are separate criteria. The uniformity of the absorbed-dose distribution within the target volume is known as dose homogeneity. The degree to which the high-dose zone conforms to the target volume, often the PTV, is characterized by dosage conformity. Figure 2.3 represents the relationship of dose conformity and dose homogeneity (Menzel, 2010). Homogeneity index (HI) as presented in ICRU 83 is one of the dose evaluations tools and requirement for dose reporting for Intensity Modulated Radiation Therapy (IMRT) technique. An HI of zero indicates that the absorbed-dose distribution is almost homogeneous. HI is given by equation (2.1) as follows.  $D_{2\%}$  is defined as minimum dose to 2% of the target volume indicating the “maximum dose”,  $D_{98\%}$  is minimum dose to the 98% of the target volume, indicating the “minimum dose” and  $D_{50\%}$  is the normalization value.

$$HI = \frac{D_{2\%} - D_{98\%}}{D_{50\%}} \quad (2.1)$$



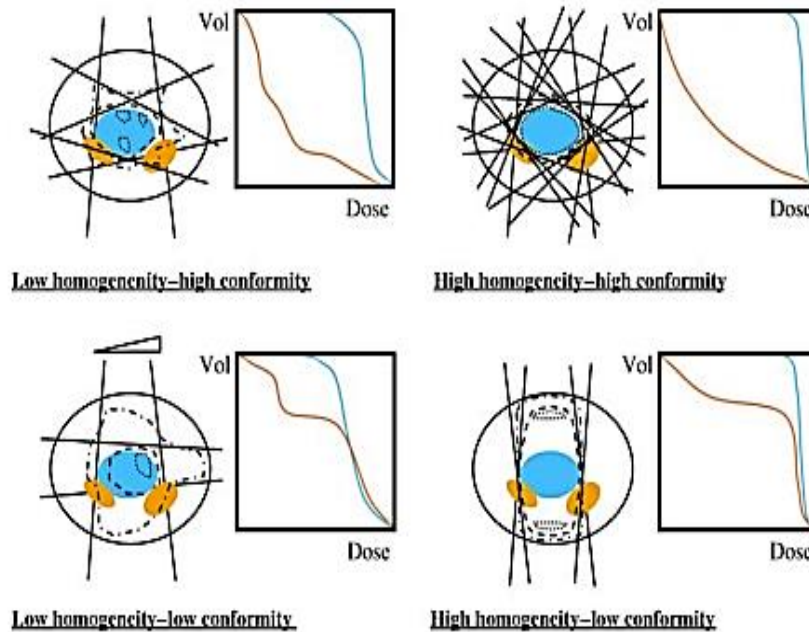


Figure 2.2: Dose homogeneity and dose conformity relationship (Barrett et al., 2009).

As reported by Barrett et al, it is recommended to report dose specification point is accompanied by a statement of the homogeneity of the irradiation as defined by at least the maximum and minimum doses to the PTV (Barrett et al., 2009). In relation to breast radiotherapy, in the Vicini et al. data which included 95 individuals, their statistical significance highlighted the significance of maintaining the best possible dose homogeneity in the breast (Vicini et al., 2002). However, the aim to achieve breast homogeneity were contradicted by the experiments of Prabhakar et al. 63% percent of the single-slice plans and 26.7% of the three-slice plans showed poor dose homogeneity. The study's other results showed that the majority of breast cancer cases require 3D planning. Additionally, it showed that patients with big breasts who receive typical tangential field radiation are more likely to encounter higher dose inhomogeneity (Prabhakar et al., 2008). So far dose homogeneity index has only been applied to IMRT technique. However, looking into the breast inhomogeneity reported in previous

literature, there's a critical demand in calculating and applying homogeneity index for 3DCRT during the course of this research.

## **2.2 Radiological and Physical Properties of Brass Mesh Bolus**

### **2.2.1 Mass Density and Electron Density**

To be deemed equivalent to tissue or water, a material should have the same amount of electrons per gramme and mass density, according to Khan and Gibbons (F. M. Khan & Gibbons, 2014). Therefore, a material's electron density can be estimated using its mass density and atomic number using the equation (2.2) where,  $\rho_e$  represent the electron density, mass density ( $\rho_m$ ), Avogadro's number ( $N_A$ ), atomic number ( $Z$ ).

$$\rho_e = \rho_m \times N_A \times \frac{Z}{A} \quad (2.2)$$

The concept of mass density and electron density in radiation therapy is related to each other. Much of the current literature on relationship of material density and electron density of respective material has become available in radiotherapy application. Earlier, Martinez et al, has documented a study where in order to make inhomogeneity corrections, it is necessary to establish a connection between tissue electron densities ( $\rho_e$ ) and the associated Hounsfield Units (HU). The selection of the tissue equivalent materials ensured that a wide range of  $\rho_e$  would be taken into account for the CT scanner calibration (Herrera-Martínez et al., 2006). The conversion of Computed Tomography (CT) values from a tomographic scan to a mass density is a crucial step in the electron Monte Carlo dosage calculation. This study by Raymond et al, examines how a calibration table between CT number and mass density might be perturbed to determine the dosimetric effects (Fang et al., 2018).